Solutions of three-particle Faddeev equations above the breakup threshold via separable expansions of two-particle resolvents in a basis of two-particle pseudostates

Zeki C. Kuruoğlu *
Department of Chemistry, Bilkent University, 06800 Bilkent, Ankara, Turkey

(Received 5 March 2024; accepted 6 May 2024; published 30 May 2024)

A separable expansion of the two-particle free resolvent in terms of two-particle pseudostates is used to convert Alt-Grassberger-Sandhas (AGS) integral equations into a set of effective two-body equations in spectator degrees of freedom. The resulting effective two-body equations are much like the multichannel Lippmann-Schwinger (LS) equations of inelastic scattering with real, energy independent, nonsingular potential matrices. Hence, they are more conducive to computations than the effective equations that ensue in the conventional approach based on separable expansions of two-particle transition operators. In particular, the problem of moving singularities of the conventional approach is avoided. The effective propagator matrix is complex and nondiagonal, and exhibits simple-pole singularities in diagonal elements corresponding to open rearrangement channels. These singularities can be handled by simple subtraction procedures well known from two-particle scattering. After regularization of the kernel, the set of coupled LS-type equations in the spectator momenta are solved rather straightforwardly via the Nyström method in which the integrals over spectator momenta are discretized using suitable quadrature rules. Solutions of effective two-body equations are then used to calculate the breakup amplitudes using the well-known relationship between rearrangement and breakup amplitudes. This proposed method has been tested on two models: (i) particle-dimer collisions in a three-boson model with s-wave separable pair potentials and (ii) an s-wave benchmark model with local pair potentials of the $n + d$ collisions. Calculations reported in the present article show that rather accurate results for elastic and breakup amplitudes can be obtained with pseudostates generated from a relatively small number of local basis functions in momentum space.

DOI: 10.1103/PhysRevC.109.054004

I. INTRODUCTION

In the context of Faddeev formalism of three-particle dynamics [1–5], the important role played by separable approximations [6–8] and expansions [9–13] of two-particle interactions is well known. For potentials representable as finite-rank expansions, the Alt-Grassberger-Sandhas (AGS) equations can be converted into Lippmann-Schwinger (LS) type multichannel integral equations in the spectator momenta [3–5]. In fact, in early phases of three-particle computations, this was, if not the only, the standard scheme to solve the Faddeev or AGS equations in momentum space (see, e.g., [14] and references therein). Computational implementation of the effective two-body integral equations of this approach, however, is impeded by the moving logarithmic singularities [4,5,15] in the effective interaction matrix. The usual method of quadrature discretization for integral equations can not be used because delicate and tedious handling [15,16] of these singularities is required. Nevertheless, this approach might still be more suitable for certain problems, although other approaches like the finite-difference [17,18] or finite element [19] methods for the differential form of Faddeev equations or numerical multivariable methods for the AGS integral equations in momentum space [15,20] dominate the current computational scene. Of course, mention must also be made of other rigorous non-Faddeev methods which are directly based on the Schrodinger equation [21–23].

That a similar scheme of reduction of three-particle dynamics into effective two-body form is possible with the use of separable expansions of the two-particle free resolvent is perhaps not appreciated commonly. Just as separable expansions of two-particle potentials lead to separable expansions of two-particle transition operators, finite-rank expansions of the two-particle free resolvents give rise to finite-rank separable expansions for the two-particle resolvents (without, however, having to approximate the two-particle interaction). It turns out that the effective two-body equations that result from using the separable expansions of the two-particle resolvents in AGS-like equations are easier to deal with. In fact, they are more like the multichannel Lippmann-Schwinger (LS) equations of inelastic collisions. The effective interaction matrix is real, energy independent, and free of singularities. The purpose of the present contribution is to explore this approach formally and computationally.

In a precursor form of this idea, two particle-Hamiltonian was approximated by its projection on a finite-dimensional approximation space, giving rise to (approximate) bound states and positive-energy pseudostates embedded in the continuum. The corresponding resolvent has a separable form in terms of bound states and pseudostates, with continuum replaced by a discrete sum over pseudostates. This idea

*kuruoglu@bilkent.edu.tr

was used in the context of the coupled-reaction-channels (CRC) ansatz and in AGS equations with very satisfactory results [22–24]. That breakup amplitudes can be computed from a discretization of two-particle continua via pseudostates is especially remarkable. The approximation of the two-particle resolvent in this manner, however, is somewhat simplistic, because both interaction and kinetic energy of the two-particle system is approximated by their projections. More sophisticated schemes of approximating two-particle resolvents exist [25,26].

One possible scheme would be to use the projection of the free resolvent on the finite-dimensional approximation space, but leave the potential intact. Note that two-particle kineticenergy is not projected by itself, rather it is the two-particle free resolvent that is replaced by its projection. The corresponding two-particle resolvent (with original potential) has a rank-N separable form, but with a nondiagonal matrix representation [25,26]. By expressing the projector in terms of bound and pseudostates, bound state poles can be localized in the diagonal elements. In the present contribution, this resolvent expansion is used in two off-shell transformed versions of the AGS equations to derive effective two-body integral equations in spectator momenta. The resulting effective two body equations resemble multichannel LS equations of inelastic scattering. The potential matrix is real and energy independent. But the propagator term is nondiagonal, energy dependent, and complex, and exhibits a simple-pole singularity as spectator momenta go through on-shell momenta of the open rearrangement channels. If n_o is the number of open rerarrangement channels at a given total energy, the on-shell transition matrix of the effective two-body problem is $n_o \times n_o$. The corresponding S matrix is not unitary, because flux loss into breakup is not explicitly represented. In effect, the propagator term absorbs the flux that would go into breakup. In other words, information about breakup is buried in half-off-shell behavior of the effective two-body transition matrix. To recover the breakup information, I use the well-known relationship between breakup and rearrangement transition operators, which in effect is equivalent to the integral formula for the breakup amplitude in terms of scattering state.

This approach is much like the resolvent approximations used in Refs. [27,28], where, however, a complete discretization is performed by projecting not only the two-particle (free and full) resolvents, but the free spectator resolvent as well. In the present case, I leave out the spectator degree of freedom as the scattering variable to be treated separately through any one of a large list of computational methods well known from two-body applications (see, e.g., Refs. [4,5,26,29]).

This article is organized as follows: Section II introduces the notation, kinematics, channel structure, and the two-particle bases to be used to generate the two-particle pseudostates. Section III is devoted to a discussion of separable expansions of two-particle resolvents. Formal aspects of the proposed approach is developed in Sec. IV. Section IV A is devoted to the review of Faddeev-AGS and Faddeev-Lovelace equations. Modified versions of AGS equations are introduced in Sec. IV B and then used in Sec. IV C to derive effective two-body equations. The procedure used to calculate the breakup amplitudes is outlined in Sec. IV D. Computational details and results are reported in Sec. V. Finally, concluding remarks are made in Sec. VI.

II. THE THREE-PARTICLE SYSTEM

The three-particle system considered in this work consists of three identical particles whose total interaction is pairwise additive. The pair potentials are restricted to act only on the s-wave states of the pairs. In addition, only states of zero total orbital angular momentum are considered. The particle (nucleon) mass and $\hbar$ are set to unity and fm is taken as the unit of length. The nucleon mass adopted yields the conversion factor 1 fm^{-2} = 41.47 MeV.

Two models are considered:

(i) The particle-dimer collision in a system of three spinless bosons. The pair potential is taken to be separable with the parameters as given in [23] and with dimer binding energy equal to binding energy of the deuteron.
(ii) A model of the $n + d$ scattering that is frequently used in the literature as benchmark for the testing of three-particle methods [17–19,21,22].

The formal structure of the proposed method of discretization will be developed and explicated for the $n + d$ model. The equations for the bosonic particle-dimer model are obtained by removing all references to spin from the equations of the $n + d$ model.

A. Kinematics, spin states, and channels

The standard three-particle notation [4,5] will be used throughout this article. The Jacobi coordinates for the arrangement α are denoted by $\mathbf{x}_\alpha$ and $\mathbf{y}_\alpha$, with the corresponding reduced masses being μ_α and ν_α, respectively. Here $\mathbf{y}_\alpha$ is the relative coordinate of the pair $(\beta\gamma)$, and $\mathbf{y}_\alpha$ the relative position of the third (spectator) particle α with respect to the center of mass of the pair $(\beta\gamma)$. The momenta conjugate to $\mathbf{x}_\alpha$ and $\mathbf{y}_\alpha$ are $\mathbf{p}_\alpha$ and $\mathbf{q}_\alpha$, respectively.

The total Hamiltonian H of the system in the center-of-mass frame is given as $H = H_0 + V$. Here, H_0 is the kinetic energy operator, and V the total interaction which is pairwise additive. H_0 can be decomposed as $H_0 = k_\alpha + K_\alpha$, where $k_\alpha = p_\alpha^2/(2\mu_\alpha)$, and $K_\alpha = q_\alpha^2/(2\nu_\alpha)$, $\alpha = 1, 2, 3$. Its eigenstates are the plane-wave states $|\mathbf{p}_\alpha\mathbf{q}_\alpha\rangle$. Restricting the present consideration to three-particle states of zero total orbital angular momentum and s-wave two-particle states, the only partial wave states of interest are $|p_\alpha q_\alpha\rangle = (4\pi)^{-1}\int d\hat{\mathbf{p}}_\alpha \int d\hat{\mathbf{q}}_\alpha\, |\mathbf{p}_\alpha\mathbf{q}_\alpha\rangle$, which are normalized as $\langle p_\alpha q_\alpha \mid p'_\alpha q'_\alpha\rangle = \delta(p - p')\,\delta(q - q')/(p^2 q^2)$. It is convenient, especially in dealing with three identical particles, to use the notation $|pq\rangle_\alpha$ to stand for $|p_\alpha = p,\ q_\alpha = q\rangle$. For instance, if one denotes with P_{123} and P_{132} the cyclic permutation operators of particle labels, then $P_{123}|pq\rangle_1 = |pq\rangle_2$ and $P_{132}|pq\rangle_1 = |pq\rangle_3$ in this notation.

The internal Hamiltonian for the pair α is $h_\alpha = k_\alpha + v_\alpha$, where v_α is the spin-dependent potential between particles β and γ. For the present study, the pair interaction v_α is assumed to operate only on s-wave states. Letting s (= 0 or 1) and

i (= 0 or 1), denote, respectively, the spin and isospin of a two-nucleon subsystem, the spin-isospin states for the αth rearrangement may be written as $\mid sSiI \rangle_\alpha$, where s (i) is the spin (isospin) of the pair α and S (= 1/2 or 3/2) the total spin, and I (= 1/2) the total isospin for the $n + d$ collision. With restriction to s waves, the Pauli principle requires $s + i = 1$. Therefore, notation for the spin-isospin states for rearrangement α can be simplified as $|sS\rangle_\alpha$, with isospin quantum numbers suppressed. The spin/isospin recoupling coefficients $\Lambda^S_{ss'} = {}_2\langle sS|s'S\rangle_1$ are $\Lambda^{1/2}_{11} = 0.25$, $\Lambda^{1/2}_{00} = 0.25$, $\Lambda^{1/2}_{01} = \Lambda^{1/2}_{10} = -0.75$ for the doublet total spin state, and $\Lambda^{3/2}_{11} = -0.5$ for the quartet total spin state.

In this notation, the pair interaction v_α has the form

$$v_\alpha \;=\; \sum_{sS} |sS\,\rangle_\alpha \; v_{\alpha s}\; {}_\alpha\langle sS| \,. \tag{1}$$

The present study uses $v_{\alpha 1}$ (spin-triplet) and $v_{\alpha 0}$ (spin-singlet) of the so-called Malfliet-Tjon I-III model [15] whose form and parameters are given in Ref. [19], which has been denominated as a benchmark model for testing computational methods. In this model, the spin-triplet potential supports just one bound state (deuteron) $|\varphi_d\rangle$ with energy ϵ_d.

The energy spectrum of the two-particle system is discretized by projection onto a finite-dimensional L^2 approximation subspace s_α which is spanned by a suitable and sufficiently large set of basis functions $|u_{\alpha n}\rangle$, $n = 1, 2, \ldots, N_\alpha$. Let π_α denote the projector onto s_α. For a given spin-isospin state of the two-particle subsystem, the eigenstates of the projected two-particle Hamiltonian $\tilde{h}_{\alpha s} = \pi_\alpha h_{\alpha s}\pi_\alpha$ are denoted by $|\phi_{sn}\rangle_\alpha$, $n = 1, 2, \ldots, N_\alpha$. The corresponding energy eigenvalues are ϵ_{sn}. For the spin-triplet case ($s = 1$), the lowest state ($n = 1$) corresponds to the deuteron bound state. It is assumed that approximation basis is large enough so that deuteron bound state $|\varphi_d\rangle_\alpha$ is described accurately. That is, $|\phi_{11}\rangle_\alpha = |\varphi_d\rangle_\alpha$ and $\epsilon_{11} = \epsilon_d$. The remaining states $|\phi_{1n}\rangle_\alpha$, $n = 2, \ldots, N_\alpha$ have positive energies and are referred to as pseudostates embedded in the continuum. For the spin-singlet case, states $|\phi_{0n}\rangle_\alpha$, $n = 1, 2, s, N_\alpha$ are all pseudostates.

The rearrangement-channel Hamiltonian is H_α ($\equiv K_\alpha + \tilde{h}_\alpha$). Restricting the present treatment to states of zero total orbital angular momentum, the eigenstates of H_α are the direct-product states $\mid \phi_{sn}\rangle_\alpha \otimes |q\rangle_\alpha \otimes |sS\rangle_\alpha$ with energies $E_{\alpha snq} = \epsilon_{sn} + 3q^2/4$. Alternative notation $\mid \phi_{sn}\, q\, sS\,\rangle_\alpha$ will also be used for these channel states. Only the channel state with $n = 1$, $s = 1$ represents a physical channel while all the rest are pseudochannels embedded in the continuum which simulate the breakup channel.

Let us denote the state space associated with the spectator particle by S^α, on which the identity operator is I^α. The direct product $s_\alpha \otimes S^\alpha$ gives the computational space $\mathcal{S}_\alpha$ for the rearrangement channel α. Projector Π_α onto $\mathcal{S}_\alpha$ is then given by the direct product $\pi_\alpha \otimes I^\alpha$. For the subspace of $\mathcal{S}_\alpha$ with total spin S, the explicit form of the projector is given by

$$\Pi^S_\alpha = \sum_{s,n} \int q^2 dq \; |\phi_{sn} q s S\rangle_\alpha \; {}_\alpha\langle \phi_{sn} q s S| \,. \tag{2}$$

As part of the notational convention, two-particle operators on s_α are denoted by lower case letters, while capital letters are used for their extension to the three-particle space $\mathcal{S}_\alpha$. In this notation, e.g., $V_\alpha = v_\alpha \otimes I^\alpha$.

Final states in the breakup channel are eigenstates of H_0 : $|pq\rangle_\alpha \otimes \mid sS\,\rangle_\alpha$ for which an alternative notation is $|pqsS\rangle_\alpha$. Of course, breakup can as well be described in terms of continuum states $|p^{(+)}qsS\rangle_\alpha$ of H_α. These continuum states satisfy

$$|p^{(+)}qsS\rangle_\alpha = W_\alpha\, |pqsS\rangle_\alpha = (I \,+\, G_0\, T_\alpha)\, |pqsS\rangle_\alpha \tag{3}$$

where W_α is the two-particle wave operator, T_α the two-particle transition operator, and $G_0(z) = (z - H_0)^{-1}$ the free resolvent.

The channel external interactions V^α are defined by $V^\alpha = H - H_\alpha$. In the discussion of three-particle theory, the following resolvent operators will also be encountered: $G(z) = (z - H)^{-1}$, $G_\alpha(z) = (z - H_\alpha)^{-1}$, $g_\alpha(z) = (z - h_\alpha)^{-1}$, and $g_{0\alpha}(z) = (z - k_\alpha)^{-1}$, $\alpha = 1, 2, 3$. The rearrangement-channel resolvent $G_\alpha(E + i0)$ in total spin state S has the spectral decomposition

$$\begin{aligned} G^S_\alpha(E + i0) = &\int q^2 dq \, \frac{|\varphi_d q s_d S\,\rangle_\alpha \; {}_\alpha\langle \varphi_d q s_d S\,|}{E - \epsilon_d - (q^2/2\nu_1) + i0} \\ &+ \sum_s \int p^2 dp \int q^2 dq \\ &\times \frac{|p^{(+)}qsS\,\rangle_\alpha \; {}_\alpha\langle p^{(+)}qsS\,|}{E - (p^2/2\mu_1) - (q^2/2\nu_1) + i0}. \end{aligned} \tag{4}$$

where $s_d = 1$.

B. Expansion basis and pseudostates for the two-particle subsystems

The two-particle pseudostates are generated using a basis with local support in momentum space. In this contribution, the primitive basis $\{u_{\alpha i}(p_\alpha)\}$ consists of local piecewise quadratic (LPQ) polynomials [30] defined over a grid in relative momentum p of the two-body system. A cutoff value $p_{\max}$ is introduced for p_α. The computational interval $[0, p_{\max}]$ is partitioned into $\mathcal{I}_p$ subintervals (finite elements), and a set of $2\mathcal{I}_p - 1$ quadratic local-interpolation functions $\zeta_i(p)$ are defined on this grid. Note that the grid does not have to be evenly distributed.

Let $\{P_1, P_2, \ldots, P_{I_p+1}\}$ be the set of break points for a partition of the interval $[0, p_{\max}]$ into I_p finite elements. Here $P_1 = 0$ and $P_{I_p+1} = P_{\max}$. The midpoint of the ith finite element $[P_i, P_{i+1}]$ is denoted $P_{i+1/2}$, $i = 1, 2, \ldots, I_1$. Collecting and ordering the break points and midpoints of all the finite elements together, I form the set $\{p_1, p_2, \ldots, p_{\tilde{N}}\}$ of grid points, where $\tilde{N} = 2I_p + 1$, $p_N = p_{\max}$, and $p_{2i-1} = P_i$, $p_{2i} = P_{i+1/2}$, for $i = 1, \ldots, I_p$. This set (to be referred to as the *grid*) provides the setting for the definition of the p basis $\{\zeta_n(p)\}$. Each basis function $\zeta_n(p)$ will be centered at its corresponding grid point p_n and will satisfy the cardinal property $\zeta_n(p_m) = \delta_{nm}$, $n, m = 1, 2, \ldots, \tilde{N}$.

These local piecewise quadratic polynomials are best described in terms of a local variable ξ, defined separately for each finite element. The finite element $[P_i, P_{i+1}]$ is mapped

to $[-1, 1]$ via $\xi = (2q - P_i - P_{i+1})/(P_{i+1} - P_i)$. In terms of the local variable s, the basis functions associated with the breakpoints read

$$\zeta_{2i-1}(p) = \begin{cases} -\xi(1-\xi)/2 & \text{for } P_i < p < P_{i+1}, \\ \xi(1+\xi)/2 & \text{for } P_{i-1} < p < P_i, \\ 0 & \text{otherwise,} \end{cases}$$

for $i = 1, 2, \ldots, I_p + 1$; while the functions associated with the midpoints of finite elements have the form

$$\zeta_{2i}(p) = \begin{cases} 1 - \xi^2 & \text{for } P_i < p < P_{i+1}, \\ 0 & \text{otherwise,} \end{cases}$$

for $i = 1, 2, \ldots, I$. These functions are depicted, e.g., in Ref. [31], where they have been used to discretize the momentum space in the context of a time-dependent wave-packet calculation. They have finite support: the ones associated with breakpoints (nodes) are nonzero over two finite elements, while those associated with midpoints of the finite elements are nonzero over one finite element.

The two-particle expansion bases are then defined as $u_i(p_\alpha) = \zeta_{i+1}(p_\alpha)/p_\alpha \quad i = 1, N$, where $N = 2I_p - 1$. Note that the local functions associated with the first and last grid points (namely ζ_1 and $\zeta_{\tilde{N}}$ have been removed.

Although the local basis $\{u_i(p_\alpha)\}$ is not orthonormal, the pseudostates generated in terms of it are orthonormal by construction.

Note that the spectrum of pseudostate energies can be varied by changing the approximation subspace s_α. Hence, the pseudostates do not represent an invariant property of the two-particle system. Nevertheless, a given set of pseudostates carry information about the continuum of the two-particle system. For a given number of grid points (and hence a given number of basis functions), the spectrum of pseudostate energies can be adjusted by changing the distribution of grid points over the computational interval $[0, p_{\max}]$ as deemed necessary.

Although piecewise quadratic basis functions were preferred in the present study, other classes of local interpolation bases (such as piecewise linear, cubic Hermite, cubic spline) or even other types of local bases (like distributed Gaussians) could be used as well. The author's experience with the the local quadratic basis to discretize the momentum variables has been rather satisfactory in such scattering applications as the time-dependent wave-packet propagation [31–33] and in the context of multivariable discretization needed for the solution of two- and three-dimensional LS equations without angular momentum decomposition [26,29].

III. SEPARABLE EXPANSIONS FOR THE TWO PARTICLE RESOLVENT

In the most straightforward use of pseudostates, the two-particle resolvent g_α is approximated by

$$g_\alpha \approx \pi_\alpha (z\pi_\alpha - \pi_\alpha h_\alpha \pi_\alpha)^{-1} \pi_\alpha \,. \tag{5}$$

That is, in the spectral decomposition, the integral over continuum states is replaced by a discrete sum over pseudostates. $G_\alpha(E + i0)$ is then approximated as

$$G^S_\alpha(E + i0) \approx \left[E + i0 - \Pi^S_\alpha H_\alpha \Pi^S_\alpha\right]^{-1} = \sum_s \sum_n \int q^2 dq \, \frac{|\phi_{sn} qsS\rangle_\alpha \, {}_\alpha\langle \phi_{sn} qsS|}{E - \epsilon_{sn} - (q^2/2\nu_1) + i0}. \tag{6}$$

This type of approach has been used in the CRC ansatz and in the AGS equations with satisfactory results [22–24].

Other resolvent approximations are possible on the finite subspace s_α spanned by the the two-particle pseudostates. For example, the two-particle free resolvent $g_{0\alpha}$ can be approximated by its projection onto the two-particle approximation space s_α:

$$\tilde{g}_{0\alpha} = \pi_\alpha g_{0\alpha} \pi_\alpha, = \sum_n \sum_{n'} |\phi_n\rangle \, (\tilde{\mathbf{g}}_{0\alpha})_{nn'} \, {}_\alpha\langle \phi_{n'}|, \tag{7}$$

where the matrix $\tilde{\mathbf{g}}_{0\alpha}$ is given by

$$(\tilde{\mathbf{g}}_{0\alpha})_{nn'} =_\alpha \langle \phi_n | g_{0\alpha} | \phi_{n'} \rangle_\alpha = \int p^2 \, dp \, \frac{\phi_{\alpha n}(p) \, \phi_{\alpha n'}(p)}{z - p^2/(2\mu)}. \tag{8}$$

The corresponding two-particle resolvent $\tilde{g_\alpha}$ is the solution of the resolvent LS equation $\tilde{g}_\alpha = \tilde{g}_{0\alpha} + \tilde{g}_{0\alpha} \, v_\alpha \tilde{g}_\alpha$. For the two-particle spin state s, one finds that

$$\tilde{g}_{\alpha s} = \tilde{g}_{0\alpha} \left[\tilde{g}_{0\alpha} - \tilde{g}_{0\alpha} v_{\alpha s} \tilde{g}_{0\alpha}\right]^{-1} \tilde{g}_{0\alpha} \tag{9}$$

In explicit form

$$\tilde{g}_{\alpha s} = \sum_n \sum_{n'} |\phi_{ns}\rangle_\alpha \, (\tilde{\mathbf{g}}_{\alpha s})_{nn'} \, {}_\alpha\langle \phi_{n's}|, \tag{10}$$

where the matrix $\tilde{\mathbf{g}}_{\alpha s}$ is defined by

$$\tilde{\mathbf{g}}_{\alpha s} = \left[\tilde{\mathbf{g}}^{-1}_{0\alpha} - \mathbf{v}_{\alpha s}\right]^{-1} \tag{11}$$

with $(\mathbf{v}_{\alpha s})_{nn'} =_\alpha \langle \phi_{ns} | v_{\alpha s} | \phi_{n's} \rangle_\alpha$.

The channel resolvent $G_\alpha(E + i0)$ is then approximated as

$$G^S_\alpha(E + i0) \approx \sum_s \sum_n \sum_{n'} \int q^2 dq \, |\phi_{sn} qsS\rangle_\alpha \times (\tilde{\mathbf{g}}_{\alpha s}(E^+_q))_{nn'} \, {}_\alpha\langle \phi_{sn'} qsS|, \tag{12}$$

where E^+_q stands for $z = E - q^2/(2\nu_\alpha) + i0$.

Equation (12) represents the separable expansion of the two-particle resolvent that will be used in the present study to derive effective two-body equations for the spectator degrees of freedom. Note that bound states appear as simple poles in corresponding diagonal elements of $\tilde{\mathbf{g}}_{\alpha s}$, while pseudostates do not give rise to any singularities. This last point is an interesting aspect of the present approach. It is to be contrasted with Eq. (6) where pseudostates give rise to singularities which in turn define pseudo-rearrangement channels. In Eq. (12), the effective propagator $\tilde{\mathbf{g}}_{\alpha s}(E^+_q)$ is nondiagonal, complex, and energy dependent, while vertex states are real. For values of E_q in the immediate vicinity of the bound-state energies, the usual pole behavior is recovered in the corresponding diagonal element. Of course, $\tilde{\mathbf{g}}_{\alpha s}(E^+_q)$ could be brought into diagonal form, but at the price of making the

vertex states energy dependent and complex. This is not desirable because it would mean back to the problem of moving logarithmic singularities that one would like to avoid.

Other separable expansions of $g_{0\alpha}$ can be generated via one-sided projections $\pi_\alpha g_{0\alpha}$ and $g_{0\alpha}\pi_\alpha$. An even more efficient scheme is the symmetric construction $g_{0\alpha}\,\pi_\alpha\,[\,\pi_\alpha\,g_{0\alpha}\,\pi_\alpha\,]^{-1}\,\pi_\alpha\,g_{0\alpha}$. This last type of projection is called *inner projection* in quantum chemistry literature [34]. The use of the inner projection approximation for $g_{0\alpha}$ in the resolvent equation $g_\alpha = g_{0\alpha} + g_{0\alpha}\,v_\alpha\,g_\alpha$ produces a separable expansion that is equivalent to the application of a Schwinger-like variational principle on the approximation subspace s_α [25,26]. The corresponding approximation for the rearrangement channel resolvent would read

$$G^S_\alpha(E+i0) \approx \sum_s \sum_n \sum_{n'} \int q^2 dq\; g_{0\alpha}(E^+_q)\,|\phi_{sn}qsS\,\rangle_\alpha \times \left[\mathbf{\Delta}^{-1}_{\alpha s}(E^+_q)\right]_{nn'}\,{}_\alpha\langle\phi_{sn'}qsS\,|\,g_{0\alpha}(E^+_q), \tag{13}$$

where

$$[\,\mathbf{\Delta}_{\alpha s}(E^+_q)\,]_{nn'} = {}_\alpha\langle\phi_n|g_{0\alpha}(E^+_q)|\phi_{n'}\rangle_\alpha - {}_\alpha\langle\phi_n|\,g_{0\alpha}(E^+_q)v_{\alpha s}\,g_{0\alpha}(E^+_q)\,|\phi_{n'}\rangle_\alpha\,.$$

This would definitely be a better approximation to $G^S_\alpha(E+i0)$ than the one in Eq. (12). However, the vertex states $g_{0\alpha}(E^+_q)\,|\phi_{sn}qsS\,\rangle_\alpha$ of this separable expansion are complex and energy dependent due to the presence of $g_{0\alpha}$, and that feature makes Eq. (13) less desirable for use in the AGS equations. When Eq. (13) is used in AGS equations to derive effective two-body equations, the elements of the effective potential matrix would involve integrals with moving logarithmic singularities, just as in the standard approach with separable potentials. Therefore, the resolvent expansion given in Eq. (12) is preferred in the present work.

IV. THEORETICAL DEVELOPMENT

A. Review of Faddeev formalism: AGS and Lovelace equations

For a collision starting in rearrangement 1, the Alt-Grassberger-Sandhas (AGS) version of Faddeev equations [1] for rearrangement transition operators read [3]

$$U_{\beta 1} = \bar\delta_{\beta 1}G_0^{-1} + \sum_{\gamma=1}^{3}\bar\delta_{\beta\gamma}\,T_\gamma G_0\,U_{\gamma 1}, \tag{14}$$

where $\bar\delta_{\beta\alpha} = 1 - \delta_{\beta\alpha}$. and T_γ is the transition operator for the pair potential V_γ. With $\beta = 1, 2, 3$, the above equations form a closed set of equations for U_{11}, U_{21}, and U_{31}. The breakup transition operator is then given as

$$U_{01} = G_0^{-1} + T_1G_0\,U_{11} + T_2G_0\,U_{21} + T_3G_0\,U_{31}, \tag{15}$$

which can also be reexpressed as

$$U_{01} = G_0^{-1}\delta_{\gamma 1} + (I + T_\gamma G_0)U_{\gamma 1} = G_0^{-1}\delta_{\gamma 1} + W^\dagger_\gamma U_{\gamma 1}, \tag{16}$$

where γ can be 1, 2, or 3, and the subsystem wave operator W_γ is the solution of $W_\gamma = I + G_0V_\gamma W_\gamma$ and satisfies $W_\gamma = I + G_0T_\gamma = I + G_\gamma V_\gamma$. Note that, the G_0^{-1} term in Eq. (14) does not contribute to the on-shell breakup amplitudes.

Another version of Faddeev equations that has received lesser attention in applications is the Lovelace equations (for the post-form transition operators) [2]:

$$U^{(+)}_{1\beta} = V^1 + \sum_{\gamma=1}^{3} U^{(+)}_{1\gamma}G_0T_\gamma\bar\delta_{\gamma\beta}. \tag{17}$$

The post and AGS forms of the rearrangement operators are related by $U_{\beta\alpha} = \bar\delta_{\beta\alpha}\,G_\alpha^{-1} + U^{(+)}_{\beta\alpha}$. Lovelace equations have the same kernel as the AGS equations, but the driving term differs. The solution of Lovelace equations can be obtained from those of the AGS equations by a quadrature [23]:

$$U^{(+)}_{\beta 1} = V^{(\beta)}\sum_{\gamma=1}^{3}[\delta_{\beta\gamma} + G_0T_\gamma G_0U_{\gamma,1}\,], \tag{18}$$

where the term in the parentheses is the wave operator for the γth Faddeev component of the full scattering state with initial arrangement (1). As such, this equation is nothing but the integral formula for the rearrangement operator $U^{(+)}_{\beta 1}$, viz., $U^{(+)}_{\beta 1}|\Phi_1\rangle = V^\beta|\Psi\rangle$, with $|\Psi\rangle$ standing for the full scattering state for a collision starting in the initial state $|\Phi_1\rangle$ in rearrangement (1).

The post form of the breakup transition operator is defined as

$$U^{(+)}_{01} = V + V\,G(z)V^1, \tag{19}$$

and satisfies $U^{(+)}_{01} = W^\dagger_\beta U^{(+)}_{\beta 1}$, with $\beta = 1$, 2, or 3, in analogy with Eq. (16).

For the three-nucleon case, taking rearrangement 1 as the reference rearrangement, the properly antisymmetrized form of rearrangement transition operators are

$$\mathrm{U} = U_{11} + P_{132}\,U_{21} + P_{123}\,U_{31}, \tag{20}$$

$$\mathrm{U}^{(+)} = U^{(+)}_{11} + P_{132}\,U^{(+)}_{21} + P_{123}\,U^{(+)}_{31}\,. \tag{21}$$

The antisymmetrized versions of AGS and Lovelace equations become

$$\mathrm{U} = (P_{123} + P_{132})\,G_0^{-1} + (P_{123} + P_{132})\,T_1\,G_0\,\mathrm{U}, \tag{22}$$

$$\mathrm{U}^{(+)} = (P_{123} + P_{123})\,V^1 + \mathrm{U}^{(+)}(P_{123} + P_{132})\,G_0\,T_1\,. \tag{23}$$

Here it is tacitly assumed that these equations will be used in conjunction with channel states that are antisymmetric under P_{23}. In analogy with Eq. (14), solution of Eq. (19) can be constructed from the solution of Eq. (18) :

$$\mathrm{U}^{(+)} = V^1\,(I + P_{123} + P_{123})(I + G_0\,T_1\,G_0\,\mathrm{U}). \tag{24}$$

As all rearrangements are indistinguisable from the initial rearrangement (taken as 1) and since there is just one channel state in each rearrangement of the three-nucleon system, the antisymmetric combination of rearrangement amplitudes will be referred to as the elastic amplitude.

Properly antisymmetrized transition operators into the breakup channel are given as

$$\mathrm{U}_{\mathrm{bup}} = W_1^\dagger \,\mathrm{U} \;\; = (I + T_1\, G_0)\,\mathrm{U}, \tag{25}$$

$$\mathrm{U}^{(+)}_{\mathrm{bup}} = W_1^\dagger \,\mathrm{U}^{(+)} = (I + T_1\, G_0)\,\mathrm{U}^{(+)}, \tag{26}$$

where I dropped from $\mathrm{U}_{\mathrm{bup}}$ a term that vanishes for on-shell breakup amplitudes.

B. Off-shell transformed AGS equations

To facilitate the use of separable expansions of the two-particle resolvents in three-particle context, I introduce the following off-shell transformed forms of the rearrangement operators:

$$\mathrm{A}_{\beta\alpha} = V_\beta\, G_0\, U_{\beta\alpha} \quad \text{and} \quad \mathrm{T}_{\beta\alpha} = U_{\beta\alpha}\, G_0\, V_\alpha\,. \tag{27}$$

For a collision starting in rearrangement 1, the AGS equations for these off-shell modified rearrangement operators become

$$\mathrm{A}_{\beta 1} = V_\beta\, \bar{\delta}_{\beta 1} + \sum_{\gamma=1}^{3} V_\beta \bar{\delta}_{\beta\gamma}\, G_\gamma\, \mathrm{A}_{\gamma 1}, \tag{28}$$

$$\mathrm{T}_{\beta 1} = \bar{\delta}_{\beta 1}\, V_1 + \sum_{\gamma=1}^{3} \bar{\delta}_{\beta\gamma}\, V_\gamma\, G_\gamma\, \mathrm{T}_{\gamma 1}\,. \tag{29}$$

Operators $\mathrm{A}_{\beta 1}$ and $\mathrm{T}_{\beta 1}$ are half-on-shell equivalent to $U_{\beta 1}$. These operators and the above equations have been discussed in some detail in Ref. [35] and have been used for computations in Ref. [23]. Some insight into the nature of these equations can be gained by considering the wave-function counterparts of Eqs. (28) and (29). Letting $|\Phi_1\rangle$ denote the initial state, the wave-function equations are

$$\left|\psi^F_\beta\right\rangle = |\Phi_1\rangle\, \delta_{\beta 1} + \sum_{\gamma=1}^{3} G_\beta\, V_\beta \bar{\delta}_{\beta\gamma}\, \left|\psi^F_\gamma\right\rangle, \tag{30}$$

$$|\Psi_\beta\rangle \;= |\Phi_1\rangle\, \delta_{\beta 1} + \sum_{\gamma=1}^{3} G_\beta\, \bar{\delta}_{\beta\gamma}\, V_\gamma\, |\Psi_\gamma\rangle\,. \tag{31}$$

Note that $\{|\psi^F_1\rangle, |\psi^F_2\rangle, |\psi^F_3\rangle, \}$ are the Faddeev components and Eq. (30) represents the original Faddeev equations. On the other hand, $|\Psi_1\rangle$, $|\Psi_2\rangle$, and $|\Psi_3\rangle$, are each equal to the total scattering state. Thus, as $y_\beta \to \infty$, the asymptotic form of Faddeev component $|\psi^F_\beta\rangle$ yields the on-shell matrix elements of $\mathrm{A}_{\beta 1}$, while the asymptotic analysis of $|\Psi_\beta\rangle$ produces on-shell matrix elements of $\mathrm{T}_{\beta 1}$.

Introducing the antisymmetrized versions of these operators via

$$\mathrm{A} = \mathrm{A}_{11} + P_{132}\,\mathrm{A}_{21} + P_{123}\,\mathrm{A}_{31}, \tag{32}$$

$$\mathrm{T} = \mathrm{T}_{11} + P_{132}\,\mathrm{T}_{21} + P_{123}\,\mathrm{T}_{31}, \tag{33}$$

one finds that

$$\mathrm{A} = V_1\, G_0\, \mathrm{U} \;\text{ and }\; \mathrm{T} = \mathrm{U}\, G_0\, V_1\,. \tag{34}$$

The antisymmetrized AGS equation, Eq. (22), is now replaced by

$$\mathrm{A} = V_1\,(P_{123} + P_{132}) + V_1\,(P_{123} + P_{132})\, G_1\, \mathrm{A}, \tag{35}$$

$$\mathrm{T} = (P_{123} + P_{132})\, V_1 + (P_{123} + P_{132})\, V_1\, G_1\, \mathrm{T}. \tag{36}$$

These equations are of the Lipmmann-Schwinger form and are especially suitable for use in conjunction with separable approximations or expansions of the two-particle resolvent G_1. Note that interaction terms $V_1\,(P_{123} + P_{132})$ and $(P_{123} + P_{132})\,V_1$ are transposes of each other. On-shell matrix elements of A, T, and U are equal by definition. On the other hand, U^+ can be obtained from A via

$$\mathrm{U}^{(+)} \;= V^1\,(I + P_{123} + P_{123})(I + G_1\,\mathrm{A}), \tag{37}$$

which amounts to a rewriting of Eq. (24) using $\mathrm{A} = V_1\, G_0\, \mathrm{U}$.

The antisymmetrized versions of wave-function Eqs. (30) and (31) read

$$|\psi^F\rangle = |\Phi_1\rangle + G_1\, V_1 (P_{123} + P_{123})|\psi^F\rangle, \tag{38}$$

$$|\Psi\rangle = |\Phi_1\rangle + G_1\,(P_{123} + P_{123})\, V_1 |\Psi\rangle, \tag{39}$$

where $|\psi^F\rangle$ is the antisymmetrized Faddeev component and $|\Psi\rangle$ is the antisymmetrized total scattering state.

C. Effective two-body equations

In the proposed approach, separable expansion of G_1 given in Eq. (12) is used in Eqs. (35) and (36) to obtain

$$\begin{aligned}\mathrm{A}^S_{sn,11}(q,\bar{q}_{11}) = {}& \mathrm{V}^S_{sn,11}(q,\bar{q}_{11}) \\ & + \sum_{s'n'n''} \int q'^2 dq' \mathrm{V}^S_{sn,s'n'}(q,q') \\ & \times (\tilde{\mathbf{g}}_{1s'}(E^+_q))_{n'n''} \mathrm{A}^S_{s'n'',11}(q',\bar{q}_{11}),\end{aligned} \tag{40}$$

$$\begin{aligned}\mathrm{T}^S_{sn,11}(q,\bar{q}_{11}) = {}& \mathrm{V}^S_{11,sn}(\bar{q}_{11},q) \\ & + \sum_{s'n'n''} \int q'^2 dq' \mathrm{V}^S_{s'n',sn}(q',q) \\ & \times (\tilde{\mathbf{g}}_{1s'}(E^+_q))_{n'n''} \mathrm{T}^S_{s'n'',11}(q',\bar{q}_{11}),\end{aligned} \tag{41}$$

for the half-off-shell amplitudes $\mathrm{A}^S_{sn,11}(q,\bar{q}_{11})$ and $\mathrm{T}^S_{sn,11}(q,\bar{q}_{11})$ defined by

$$\begin{aligned}\mathrm{A}^S_{sn,11}(q,\bar{q}_{11}) &= {}_1\langle\phi_{sn} q s S|\,\mathrm{A}\,|\phi_{11}\bar{q}_{11} s_0 S\rangle_1, \\ \mathrm{T}^S_{sn,11}(q,\bar{q}_{11}) &= {}_1\langle\phi_{sn} q s S|\,\mathrm{T}\,|\phi_{11}\bar{q}_{11} s_0 S\rangle_1,\end{aligned} \tag{42}$$

where $s_0 = 1$, $\phi_{11} = \varphi_d$, $\bar{q}_{11} = [4(E - \epsilon_{11})/3]^{1/2}$. The momentum value $\bar{q}_{11}$ is the incident spectator momentum. Eqs. (40) and (41) are much like multichannel LS equations (in spectator degrees of freedom) with the potential matrix

$$\mathrm{V}^S_{sn,s'n'}(q,q') = {}_1\langle\phi_{sn} q s S|\, V_1\,(P_{123} + P_{132})|\phi_{s'n'} q' s' S\rangle_1\,. \tag{43}$$

Note that the effective potential matrix of the T-equation is the transpose of the effective potential matrix of the A equation, i.e., ${}_1\langle\phi_{ns} q s S|(P_{123} + P_{132})V_1|\phi_{n's'} q' s' S\rangle_1 = {}_1\langle\phi_{n's'} q' s' S|V_1(P_{123} + P_{132})|\phi_{ns} q s S\rangle_1$. Thereby, $\mathrm{T}^S_{sn,11}(q,\bar{q}_{11}) = \mathrm{A}^S_{11,sn}(\bar{q}_{11},q)$. Thus, the physical

on-shell amplitudes $\mathrm{A}^S_{11,11}(\bar{q}_{11},\bar{q}_{11})$ and $\mathrm{T}^S_{11,11}(\bar{q}_{11},\bar{q}_1)$ are the same, but off-shell amplitudes $\mathrm{A}^S_{sn,11}(q,\bar{q}_{11})$ and $\mathrm{T}^S_{sn,11}(q,\bar{q}_{11})$ differ. This is in line with the observation made after Eqs. (30) and (31), namely, that A is linked with the antisymmetrized Faddeev component, whereas T has to do with the antisymmetrized total scattering state.

The on-shell matrix element $\mathrm{A}^S_{11,11}(\bar{q}_{11},\bar{q}_{11})$ is referred to as the elastic amplitude and denoted as $\mathrm{A}_{\rm el}$. The normalization convention used is such that the elastic amplitude at total energy $E=\epsilon_d+\bar{q}^2_{11}/(2\nu_1)$ is given in terms of phase shift δ as

$$\mathrm{A}_{\rm el} = \mathrm{A}^S_{11,11}(\bar{q}_{11},\bar{q}_{11}) = \frac{-\tan\delta\, e^{i\delta}}{\pi\,\nu_1\bar{q}_{11}}\,. \tag{44}$$

The corresponding S-matrix element is $S_{\rm el}=e^{2i\delta}$. Similar statements hold for $\mathrm{T}_{\rm el}\equiv\mathrm{T}^S_{11,11}(\bar{q}_{11},\bar{q}_{11})$.

The kernels of Eqs. (40) and (41) have a simple-pole singularity at $q'=q_{11}$, corresponding to the antisymmetrized elastic channel. After an appropriate regularization of this fixed-point singularity as described in Ref. [36], effective two-body equations are solved by quadrature discretization (Nyström method) [37]. It is remarkable that there are no poles corresponding to pseudochannels. That is, the on-shell A and T matrices are 1×1. Since the potential matrix is real, flux loss into the breakup channel must take place through the propagator term $\tilde{\mathbf{g}}_{\alpha s}(z)$. All amplitudes $\mathrm{A}^S_{sn,11}(q,\bar{q}_{11})$ and $\mathrm{T}^S_{sn,11}(q,\bar{q}_{11})$ other than $\mathrm{A}^S_{11,11}(\bar{q}_{11},\bar{q}_{11})$ and $\mathrm{T}^S_{sn,11}(\bar{q}_{11},\bar{q}_{11})$ are non-physical amplitudes which, however, carry information about transitions into the breakup channel. In contrast, in the pseudostate discretization of the AGS equations via Eq. (6) [23], every energetically accessible pseudostate gives rise to a pseudochannel, and on-shell A and A matrices are $N_o\times N_o$, where N_o is the number of open pseudochannels.

Elastic amplitude can also be calculated as the on-shell matrix element of $\mathrm{U}^{(+)}$, viz.,

$$\mathrm{U}^{(+)S}_{sn,11}(q,\bar{q}_{11}) \;=\; {}_1\langle\phi_{sn}qsS|\,\mathrm{U}^{(+)}\,|\phi_{11}\bar{q}_{11}s_0S\rangle_1\,.$$

One can construct it using the solution of Eq. (40) in Eq. (37):

$$\begin{aligned}\mathrm{U}^{(+)S}_{sn,11}(q,\bar{q}_{11}) \;=\; & \mathrm{V}^{(+)S}_{sn,11}(q,\bar{q}_{11}) \\ & + \sum_{s'n'n''}\int q'^2\,dq'\,\mathrm{V}^{(+)S}_{sn,s'n'}(q,q') \\ & \times(\tilde{\mathbf{g}}_{1s'}(E^+_q))_{n'n''}\,\mathrm{A}^S_{s'n'',11}(q',\bar{q}_{11}),\end{aligned} \tag{45}$$

where $\mathrm{V}^{(+)S}_{sn,s'n'}(q,q')={}_1\langle\phi_{sn}qsS|V^1(I+P_{123}+P_{132})|\phi_{s'n'}q's'S\rangle_1$.

D. Computation of breakup amplitudes

The connection between $\mathrm{U}_{\rm bup}$ and U, as given in Eq. (25), leads us to define a breakup operator $\mathrm{A}_{\rm bup}$ via

$$\mathrm{A}_{\rm bup} = T_1\,G_0\,\mathrm{U}\,. \tag{46}$$

In view of Eqs. (22) and (25), one finds that

$$\mathrm{A}_{\rm bup} = (I\;+\;T_1\,G_0)\,\mathrm{A} = W_1^\dagger\,\mathrm{A}\,. \tag{47}$$

The on-shell matrix element of the operator $\mathrm{A}_{\rm bup}$ is the so-called single component breakup amplitude that comes out from the asymptotic analysis of the antisymmetrized Faddeev component $|\psi^F\rangle$. Using Eq. (22) in Eq. (25), one finds that the total breakup amplitude can be expressed as

$$\mathrm{U}_{\rm bup} = \mathrm{U}\;+\;\mathrm{A}_{\rm bup}\;=(I+P_{123}\;+\;P_{132})\,\mathrm{A}_{\rm bup}\,. \tag{48}$$

On the other hand, in analogy with Eq. (26), if one defines another breakup operator $\mathrm{T}_{\rm bup}$ via

$$\mathrm{T}_{\rm bup}\;=W_1^\dagger\,\mathrm{T}=(I\;+\;T_1\,G_0)\,\mathrm{T}, \tag{49}$$

one finds that its relation to $\mathrm{U}_{\rm bup}$ is given by $\mathrm{T}_{\rm bup}=\mathrm{U}_{\rm bup}\,G_0\,V_1$. That is, $\mathrm{U}_{\rm bup}$ and $\mathrm{T}_{\rm bup}$ are half-onshell equivalent. Therefore,

$$\mathrm{A}_{\rm bup}\,|\phi_{11}\bar{q}_{11}s_0S\rangle_1\;=\;T_1\,G_0\,\mathrm{T}\,|\phi_{11}\bar{q}_{11}s_0S\rangle_1\,. \tag{50}$$

Nyström solutions of Eqs. (40) and (41) produce, respectively, $\mathrm{A}^S_{sn,11}(q,\bar{q}_{11})$ and $\mathrm{T}^S_{sn,11}(q,\bar{q}_{11})$ for values of q on a quadrature grid. Let $\mathrm{A}^{sS}_{\rm bup}(\theta)$ denote the single-component breakup amplitude for transition into the final breakup state $|p\,q\,sS\rangle_1$ from the initial state $|\varphi_d\bar{q}_{11}\,s_0S\rangle_1$, i.e., $\mathrm{A}^{sS}_{\rm bup}(\theta)={}_1\langle pqsS\,|\mathrm{A}_{\rm bup}\,|\phi_{11}\bar{q}_{11}s_0S\rangle_1$. This amplitude can be constructed via Eq. (47):

$$\mathrm{A}^{sS}_{\rm bup}(\theta)\;={}_1\langle pqsS\,|(I\;+\;T_1\,G_0)\,\Pi^S_1\,\mathrm{A}\,|\phi_{11}\bar{q}_{11}s_0S\rangle_1, \tag{51}$$

where p and q can take values subject to $E=p^2+3q^2/4=\epsilon_d+3\,\bar{q}^2_{11}/4$ and hyperspherical angle θ is defined by $p=\sqrt{E}\,\cos\theta$. As the solution of Eq. (40) produces only the matrix elements $\mathrm{A}^S_{sn,11}(q,\bar{q}_{11})$, the operator A in Eq. (47) has to be approximated by $\Pi^S_1\,\mathrm{A}$. The amplitude $\mathrm{A}_{\rm bup}(\theta)$ is then given as

$$\begin{aligned}\mathrm{A}^{sS}_{\rm bup}(\theta)\;=\; & \sum_n \phi_{sn}(p)\,\mathrm{A}^S_{sn,11}(q,\bar{q}_{11}) \\ & + \sum_{n'}\,{}_1\langle p|\,t_{1s}(E_q)\,g_0(E_q)\,|\phi_{sn'}\rangle_1\,\mathrm{A}^S_{sn',11}(q,\bar{q}_{11})\,.\end{aligned} \tag{52}$$

where $t_{1s}(E_q)$ is the two-particle t-operator for the pair potential v_{1s} at the two-particle energy $E_q=E-3q^2/4$.

On account of Eq. (50), the amplitude $\mathrm{A}^{sS}_{\rm bup}$ can also be constructed from the solution of Eq. (41):

$$\mathrm{A}^{sS}_{\rm bup}(\theta)\;=\;\sum_{n'}\,{}_1\langle p|\,t_{1s}(E_q)\,g_0(E_q)\,|\phi_{sn'}\rangle_1\,\mathrm{T}^S_{sn',11}(q,\bar{q}_{11})\,. \tag{53}$$

In view of Eq. (22) and in analogy to Eq. (37), the solutions $\mathrm{U}^{(+)sS}_{sn',11}(q,\bar{q}_{11})$ of the Lovelace equation provide yet another route to the breakup amplitude. Defining $\mathrm{A}^{(+)}_{\rm bup}\;(\equiv\;T_1\,G_0\,\mathrm{U}^{(+)}_{\rm bup})$, one finds

$$\mathrm{A}^{(+)sS}_{\rm bup}(\theta)\;=\;\sum_{n'}\,{}_1\langle p|\,t_{1s}(E_q)\,g_0(E_q)\,|\phi_{sn'}\rangle_1\,\mathrm{U}^{(+)sS}_{sn',11}(q,\bar{q}_{11})\,. \tag{54}$$

In the computational implementations of Eqs. (52)–(54), the two-particle transition operator $t_{1s}(E_q)$ is constructed via the Schwinger variational principle using the pseudostate

basis. The desired matrix element becomes

$$
{}_1\langle p|\, t_{1s}(E_q)\, g_0(E_q)\, |\phi_{sn'}\rangle_1 = \sum_{n''} {}_1\langle p|\, v_{1s}\, |\phi_{sn}\rangle_1\, (\mathbf{d}_{1s})_{nn''}\, {}_1\langle \phi_{sn''}|\, v_{1s}\, g_0(E_q)\, |\phi_{sn'}\rangle_1, \tag{55}
$$

where

$$
(\mathbf{d}_{1s}^{-1})_{nn'} = {}_1\langle \phi_{sn}|\, v_{1s} - v_{1s}\, g_0(E_q)\, v_{1s}\, |\phi_{sn'}\rangle_1 . \tag{56}
$$

V. CALCULATIONS AND RESULTS

A. Details about computational implementation

In the present article, elastic amplitudes are calculated three ways, namely, by solving the integral Eqs. (40) and (41) to obtain $A^S_{11,11}(\bar{q}_{11}, \bar{q}_{11})$ and $T^S_{11,11}(\bar{q}_{11}, \bar{q}_{11})$, respectively, and by using the solution of Eq. (40) in Eq. (45) to obtain $U^{(+)S}_{11,11}$. Amplitudes $A^S_{11,11}(\bar{q}_{11}, \bar{q}_{11})$ and $T^S_{11,11}(\bar{q}_{11}, \bar{q}_{11})$ come out numerically equal within the machine accuracy, while $U^{(+)S}_{11,11}$ results are in general more accurate. Similarly, Eqs. (52), (53), and (54) provide three distinct routes to the breakup amplitudes, with the results being of very similar quality (although not identical).

Usually a division of the computational interval $[0, p_{\max}]$ into 40–50 finite elements provided sufficient accuracy. The cutoff value $p_{\max} = 12$ fm^{-1} for the two-particle momentum p proved adequate. A typical p grid for $E_{\rm lab} = 14.1$ MeV, consists of 41 finite elements with the grid points distributed as [0(14)0.45], [0.45(12)1.0], [1.0(5)1.6], 1.6(4)2.5], [2.5(3)4.0], [4.0(3)12.0], where $[a(n)b]$ means that the interval $[a, b]$ is divided into n equal finite elements. This gives rise to $N = 81$ local piecewise quadratic (LPQ) basis functions in the p variable. In the present work, for a given basis size N, all the pseudostates were included in the expansion of the two-particle resolvent.

The coupled set of effective two-body equations, Eqs. (40) or (41), contain only fixed-point singularities, which are first regularized using a multichannel version of the Kowalski-Noyes method [36]. The resulting set of nonsingular equations are then solved by quadrature discretization. A cutoff $q_{\max}$ is introduced for the upper limit of the q integrals. The value $q_{\max} = 8.0$ fm^{-1} was found to be adequate. The interval $[0, q_{\max}]$ is divided into a number of subintervals, and a Gauss-Legendre rule is applied on each subinterval. Typically a total of 150 quadrature points used for the variable q. Thus, for the calculations of the doublet state of the $n + d$ model with $N = 81$, the dimension of the linear system of complex equations that results from the Nyström method is 24300.

In Eq. (8) and in Eqs. (52)–(56), matrix elements like ${}_\alpha\langle\phi_n|g_{0\alpha}|\phi_{n'}\rangle_\alpha\langle\phi_{sn}|v_{1s}g_0(E_q)|\phi_{sn'}\rangle$ and $\langle\phi_{sn}|v_{1s}g_0(E_q)v_{1s}|\phi_{sn'}\rangle$ imply integrals with fixed-point singularities over the two-particle momentum. These are first regularized by subtraction. The nonsingular integrals are then performed using a composite Gauss-Legendre quadrature over the computational interval $[0, p_{\max}]$, typically using 16 points per finite element interval.

The amplitude commonly used in the literature [17,18,21,27,38] to present breakup results is denoted

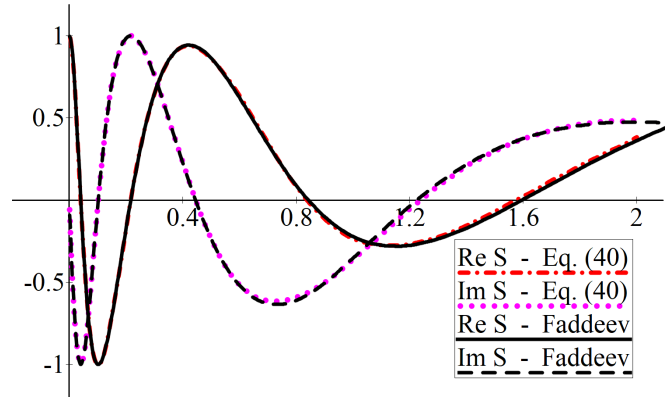

FIG. 1. Real and imaginary parts of the elastic S matrix $S_{\rm el}$ vs the incident spectator momentum $\bar{q}_{11}$ (in units of fm^{-1}) for the three-boson model with separable pair potential. Results obtained via Eq. (40) are compared with the reference (Faddeev) results obtained from the accurate solutions of the Faddeev-AGS equations via the standard scheme for separable pair potentials. The number of basis functions used in Eq. (40) ranges from 61 to 111, depending on the the incident momenta.

$\bar{A}^{sS}_{\rm bup}(\theta)$ and is related to the breakup amplitude $A^{Ss}_{\rm bup}(\theta)$ by

$$
\bar{A}^{sS}_{\rm bup}(\theta) = \frac{4\pi}{3\sqrt{3}}\, \bar{q}_0\, \kappa^4\, e^{i\pi/4}\, A^{sS}_{\rm bup}(\theta), \tag{57}
$$

where $E = \kappa^2 = p^2 + 3q^2/4$ and $p = \kappa\, \cos\theta$. $\bar{A}^{(+)sS}_{\rm bup}(\theta)$ is defined similarly.

B. Calculations for particle-dimer collision in a three boson model with separable pair potential

First tests of the proposed method were made on the bosonic particle-dimer collision model. The separable pair potential used is the same one as in Ref. [23]. As is well known, this model can be solved to arbitrary level of accuracy within Faddeev formalism. My reference (Faddeev) results for the separable-potential model were obtained by solving the effective two-body equations of the standard Faddeev-AGS approach via the Schwinger variational principle with the local piecewise quadratic (LPQ) basis and with careful attention paid to logarithmic singularities. In Fig. 1, real and imaginary parts of $S_{\rm el}$ obtained with a basis of local piecewise quadratic functions are compared with reference results for a wide range of incident spectator momenta $\bar{q}_{11}$ (in units of fm^{-1}). Collision energies $E_{\rm lab}$ in Fig. 1 range from 0 to about 186 MeV. The number of LPQ basis functions used to generate this plot was 61 for $q_{11} < 0.5$, 85 for $0.5 < q_{11} < 1.4$, and 111 for $q_{11} > 1.4$. Agreement with reference results over this rather large range of collision energies is quite satisfactory.

Table I gives the numerical comparison for $S_{\rm el}$ obtained at two collision energies using different number of basis functions. In this table, results designated as A are from the solution of Eq. (40), while results labeled by U^+ are obtained using Eq. (45), which is equivalent to the integral formula for the elastic amplitude in the post form. Both sets of results compare favorably with essentially exact results of Faddeev

TABLE I. Elastic S matrix for the particle-dimer collision in the three-boson model with separable pair potentials. Results obtained with various pseudostate bases at two collision energies are tabulated. Entries labeled with A are from solution of Eq. (40), while entries labeled with $U^{(+)}$ are from Eq. (45). The entries labeled as LPQ N in the table have been calculated using N local piecewise quadratic (LPQ) basis functions. Reference results labeled as Faddeev refer to the accurate solutions of the Faddeev-AGS equations via the standard scheme for separable pair potentials.

$E_{\rm lab}$ (MeV)	Basis	Method	$\lvert S_{\rm el}\rvert$	Re(δ)
14.1	LPQ 51	A	0.8450	164.95
		$U^{(+)}$	0.8549	166.07
	LPQ 61	A	0.8460	166.58
		$U^{(+)}$	0.8539	166.08
	LPQ 71	A	0.8638	166.15
		$U^{(+)}$	0.8544	166.08
	LPQ 91	A	0.8511	166.20
		$U^{(+)}$	0.8536	166.32
		Faddeev	0.8558	166.11
42.0	LPQ 61	A	0.4469	127.76
		$U^{(+)}$	0.4643	124.52
	LPQ 71	A	0.4787	126.79
		$U^{(+)}$	0.4637	124.51
	LPQ 81	A	0.4874	125.50
		$U^{(+)}$	0.4637	124.58
	LPQ 91	A	0.4838	124.62
		$U^{(+)}$	0.4621	124.54
	LPQ 101	A	0.4752	123.98
		$U^{(+)}$	0.4643	124.59
		Faddeev	0.4664	124.54

calculation. The agreement is usually slightly better for the results of U^{+} calculations.

Figure 2 shows the breakup amplitudes $\bar{A}_{\rm bup}(\theta)$ at $E_{\rm lab} = 14.1$ MeV, obtained with a finite element basis consisting of 91 local piecewise quadratic (LPQ) functions. This LPQ basis is defined on a division of the interval $[0, p_{\rm max}]$ into 46 subintervals. Figure 2(a) shows the breakup amplitudes $\bar{A}_{\rm bup}(\theta)$ obtained via Eq. (52). On the scale of these graphs, the results of the present approach are almost indistinguishable from the essentially exact Faddeev results, except for the behavior near $\theta = 90$ degrees. Also there are some slight oscillations at lower values of θ. Such oscillations have also been observed in connection with the full L^2-discretization

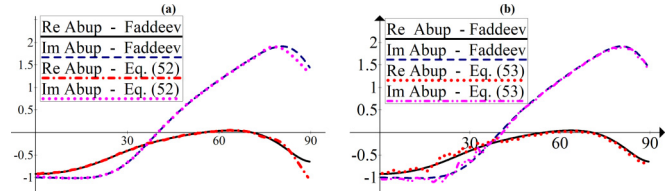

FIG. 3. Real and imaginary parts of the breakup amplitude $\bar{A}_{\rm bup}(\theta)$ vs θ (in degrees) at $E_{\rm lab} = 42$ MeV for the three-boson model with the separable pair potential. (a) $\bar{A}_{\rm bup}(\theta)$ via Eq. (52). (b) $\bar{A}_{\rm bup}(\theta)$ via Eq. (53). The number of basis functions is 101.

approach of Ref. [27] where a somewhat *ad hoc* averaging procedure was performed to smooth the results.

Figure 2(b) shows $\bar{A}_{\rm bup}(\theta)$ obtained from Eq. (53) and Fig. 2(c) gives $\bar{U}^{(+)}_{\rm bup}(\theta)$ obtained from Eq. (54). These two sets of results are not identical, but are nearly the same. If they are plotted on the same graph, they are right on top of each other on the scale of these graphs. This is not surprising because they are both extracted from the total scattering state: Eq. (53) entails the asymptotic form of the total scattering state, whereas Eq. (54) amounts to using the integral formula. In contrast, Eq. (52) refers to the asymptotic form of the Faddeev component. Comparison of Figs. 2(b) and 2(c) with Fig. 2(a) indicates that the discrepancy near 90 degrees in Fig. 2(a) is cured, but there are slightly more oscillations in Fig. 2(b) or Fig. 2(c).

Figures 3 and 5 present similar results for $E_{\rm lab} = 42$ MeV. Breakup amplitudes from Eq. (52) are in excellent agreement with Faddeev results, except for angles near 90 degrees. As before, use of Eq. (53) or Eq. (54) corrects the problem near 90 degrees, but oscillations below 40 degrees become more pronounced.

C. Calculations for the $n + d$ model

Calculations of the inelasticity and phase shift parameters of the elastic channel in the spin-doublet and spin-quartet cases are presented in Tables II and III, respectively. Results obtained via Eqs. (40) and (45) with different sizes of the LPQ basis are compared with the results available in the literature for two collision energies [17,18,21,24,38]. Agreement with benchmark results is very satisfactory. Note that in general the $U^{(+)}$ results are slightly more accurate than the A results.

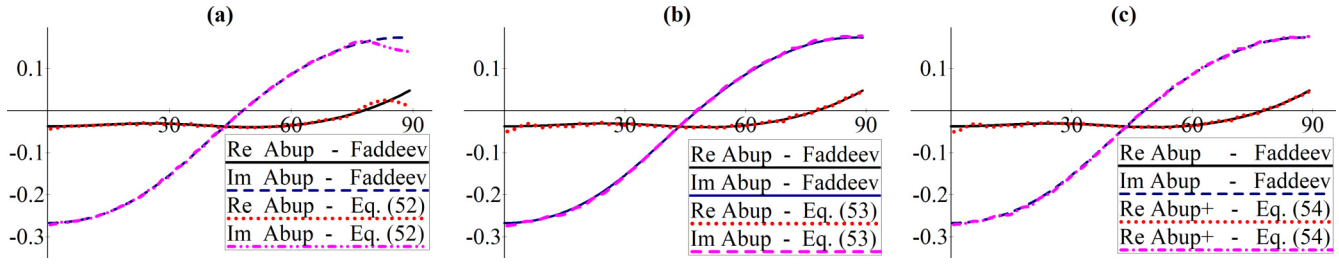

FIG. 2. Real and imaginary parts of the breakup amplitude $\bar{A}_{\rm bup}(\theta)$ vs θ (in degrees) at $E_{\rm lab} = 14.1$ MeV for the three-boson model with the separable pair potential. The breakup amplitudes obtained from present approach with a basis of 91 local piecewise quadratic (LPQ) functions are compared to the reference Faddeev results: (a) $\bar{A}_{\rm bup}(\theta)$ from Eq. (52), (b) $\bar{A}_{\rm bup}(\theta)$ from Eq. (53), and (c) $\bar{A}^{(+)}_{\rm bup}(\theta)$ from Eq. (54).

TABLE II. Real part of phase shift δ and $|S_{\rm elas}|$ for the n-d model in the spin-doublet case at two collision energies. Results obtained with various pseudostate bases are compared with the results reported in the literature. The number N of local piecewise quadratic basis functions (LPQ) used in a particular calculation is designated as LPQ N in the table. Other details are the same as in Table I.

$E_{\rm lab}$ (MeV)	Basis	Method	$\lvert S_{\rm el}\rvert$	Re(δ)
14.1	LPQ 51	A	0.4855	105.02
		$U^{(+)}$	0.4634	105.41
	LPQ 61	A	0.4541	104.92
		$U^{(+)}$	0.4630	105.42
	LPQ 71	A	0.4631	105.74
		$U^{(+)}$	0.4637	105.37
	LPQ 81	A	0.4635	105.21
		$U^{(+)}$	0.4630	105.38
		Ref. [38]	0.4648	105.48
		Ref. [17]	0.4649	105.47
		Ref. [18]	0.4648	105.40
		Ref. [21]	0.4645	105.53
		Ref. [24]	0.4658	105.30
42.0	LPQ 61	A	0.5107	39.30
		$U^{(+)}$	0.5040	41.20
	LPQ 71	A	0.4923	39.95
		$U^{(+)}$	0.5037	41.23
	LPQ 81	A	0.4874	40.78
		$U^{(+)}$	0.5032	41.20
	LPQ 91	A	0.4909	41.41
		$U^{(+)}$	0.5033	41.18
		Ref. [38]	0.5024	41.34
		Ref. [17]	0.5022	41.34
		Ref. [18]	0.5021	41.21
		Ref. [21]	0.5022	41.37
		Ref. [24]	0.5030	41.24

The breakup amplitudes $\bar{\rm A}_{\rm bup}^{1,3/2}$ in the quartet spin-state are presented in Figs. 4 and 5. Results from Eqs. (52) and (53) compare favorably with benchmark results of Ref. [38]. I do not separately show the results obtained via Eq. (54) because they are almost identical to the results obtained via Eq. (53).

It should be noted that, in the quadrature grid employed for the q variable, the quadrature point nearest to the limiting value of $\sqrt{(4E/3)}$ corresponds to about $\theta = 89$ degrees, which is the highest value of θ for which $\bar{\rm A}_{\rm bup}^{sS}$ is naturally available in the present approach. Therefore in these graphs the data for $\bar{\rm A}_{\rm bup}^{sS}$ and $\bar{\rm U}_{\rm bup}^{(+)sS}$ stops at about 89 degrees.

TABLE III. Real part of phase shift δ and $|S_{\rm elas}|$ for the n-d model in the spin-quartet case. Other details are the same as in Table II.

$E_{\rm lab}$ (MeV)	Basis	Method	$\lvert S_{\rm el}\rvert$	Re(δ)
14.1	LPQ 51	A	0.9540	70.16
		$U^{(+)}$	0.9779	68.81
	LPQ 61	A	1.0026	68.76
		$U^{(+)}$	0.9780	68.84
	LPQ 71	A	0.9691	68.58
		$U^{(+)}$	0.9755	68.89
	LPQ 81	A	0.9832	69.04
		$U^{(+)}$	0.9785	68.91
	LPQ 91	A	0.9803	68.73
		$U^{(+)}$	0.9782	68.79
	LPQ 101	A	0.9790	68.76
		$U^{(+)}$	0.9794	68.83
		Ref. [38]	0.9782	68.95
		Ref. [17]	0.9782	68.93
		Ref. [18]	0.9781	68.78
		Ref. [21]	0.9782	68.96
		Ref. [24]	0.9772	68.84
42.0	LPQ 61	A	0.9528	35.91
		$U^{(+)}$	0.9053	37.59
	LPQ 71	A	0.9106	35.96
		$U^{(+)}$	0.9033	37.68
	LPQ 81	A	0.8838	36.57
		$U^{(+)}$	0.9031	37.60
	LPQ 91	A	0.8753	37.64
		$U^{(+)}$	0.9041	37.57
	LPQ 101	A	0.8819	37.87
		$U^{(+)}$	0.9012	37.60
		Ref. [38]	0.9035	37.71
		Ref. [17]	0.9034	37.70
		Ref. [18]	0.9031	37.66
		Ref. [21]	0.9033	37.71
		Ref. [24]	0.9030	37.60

As in the three-boson separable-potential model, the $\bar{\rm A}_{\rm bup}^{1,3/2}$ results from Eq. (52) exhibit some discrepancy near the 90-degree limit. This difficulty with $\theta = \pi/2$ has been noted in other approaches [17,18,27] as well. In the present case, calculation of $\bar{\rm A}_{\rm bup}^{1,3/2}$ from Eq. (53) or calculation of $\bar{\rm U}_{\rm bup}^{(+)1,3/2}$ from Eq. (54) appears to cure this problem to a large extent, but oscillations in other regions become more pronounced.

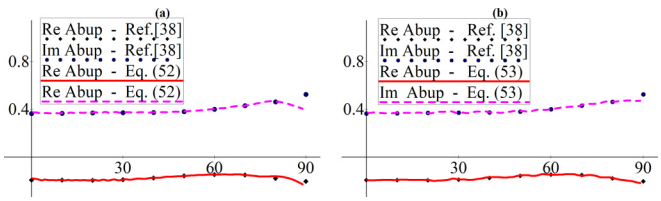

FIG. 4. Real and imaginary parts of the breakup amplitude $\bar{\rm A}_{\rm bup}(\theta)^{1,3/2}$ vs θ (in degrees) at $E_{\rm lab} = 14.1$ MeV for the $n + d$ model in the spin-quartet state. (a) $\bar{\rm A}_{\rm bup}(\theta)^{1,3/2}$ via Eq. (52). (b) $\bar{\rm A}_{\rm bup}(\theta)^{1,3/2}$ via Eq. (53). The number of basis functions is 91.

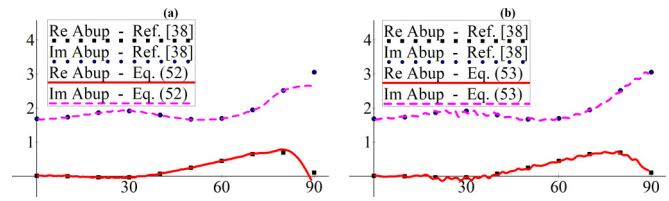

FIG. 5. Real and imaginary parts of the breakup amplitude $\bar{\rm A}_{\rm bup}(\theta)^{1,3/2}$ vs θ (in degrees) at $E_{\rm lab} = 42.0$ MeV for the $n + d$ model in the spin-quartet state. (a) $\bar{\rm A}_{\rm bup}(\theta)^{1,3/2}$ via Eq. (52). b) $\bar{\rm A}_{\rm bup}(\theta)^{1,3/2}$ via Eq. (53). Number of basis functions is 101.

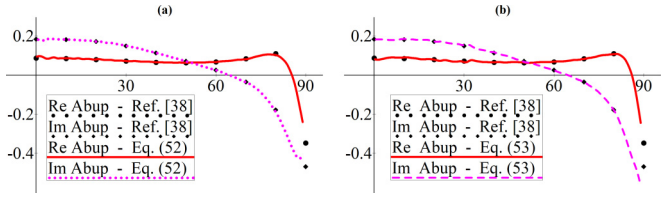

FIG. 6. Real and imaginary parts of the doublet breakup amplitude $\bar{A}_{bup}(\theta)^{0,1/2}$ vs θ (in degrees) at $E_{lab} = 14.1$ MeV for the $n+d$ model. (a)$\bar{A}_{bup}(\theta)^{0,1/2}$ via Eq. (52). (b) $\bar{A}_{bup}(\theta)^{0,1/2}$ via Eq. (53). Number of basis functions is 81.

Figures 6 and 7 present breakup amplitudes $\bar{A}_{bup}^{0,1/2}$ and $\bar{A}_{bup}^{(1,1/2}$ in the spin-doublet state at $E_{lab} = 14.1$ MeV, respectively. Finally, breakup results for the doublet state at $E_{lab} = 42$ MeV are presented in Fig. 8. Figure 8(a) shows $\bar{A}_{bup}^{0,1/2}$ while Fig. 8(b) shows $\bar{A}_{bup}^{0,1/2}$. Results obtained via both Eqs. (52) and (53) have been plotted on the same figure. They are nearly indistinguishable on the scale of these graphs. Overall, the observations and remarks made in connection with the quartet state also hold for the doublet case.

VI. CONCLUDING REMARKS

In the present work, AGS equations have been converted into LS-type effective two-body integral equations by using the separable expansion of the two-particle resolvent in a basis of pseudostates. These effective equations in the spectator momenta have more favorable properties than their counterparts that emanate from the use of separable expansions of two-particle transition operators in the AGS equations. Namely, the effective matrix interaction is real, energy independent, and free of any singularities. Therefore, it becomes possible to use any one of the standard techniques available for solving multichannel two-body LS equations [26,29,39].

Kernels of Eqs. (40) and (41) have simple poles only at two-particle bound states. For the model problems considered in this study, there is just one pole corresponding to the elastic channel. Handling of this singularity in the kernel and the selection of the quadrature grid for the Nyström method are thereby rather straightforward. However, due to the structure of the effective two-body propagator, introduction of K-matrix versions of Eqs. (40) and (41) is not computationally favorable. Therefore the Nyström method has been applied directly to Eqs. (40) and (41), giving rise to a linear system of complex

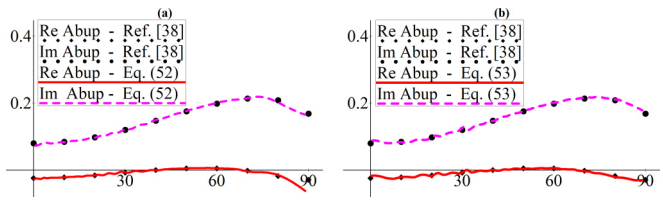

FIG. 7. Real and imaginary parts of the doublet breakup amplitude $\bar{A}_{bup}(\theta)^{1,1/2}$ vs θ (in degrees) at $E_{lab} = 14.1$ MeV for the $n+d$ model. (a) $\bar{A}_{bup}(\theta)^{1,1/2}$ via Eq. (52). (b) $\bar{A}_{bup}(\theta)^{1,1/2}$ via Eq. (53). Number of basis functions is 81.

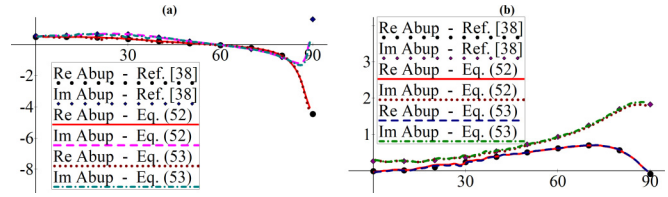

FIG. 8. Real and imaginary parts of the doublet breakup amplitudes at $E_{lab} = 42$ MeV for the $n+d$ model. (a) $\bar{A}_{bup}(\theta)^{0,1/2}$, (b) $\bar{A}_{bup}(\theta)^{1,1/2}$. The number of basis functions is 81.

equations. In contrast, in the alternative approach studied in Ref. [23], where the effective two body equations result from use of Eq. (6), the effective propagator matrix (i) has a diagonal structure with diagonal terms being of the free-resolvent form, and (ii) exhibits simple poles for both elastic and open pseudochannels. These features make the regularization of the kernel and selection of a q-quadrature grid somewhat more involved, but the introduction of K-matrix equations is straightforward and leads to a linear system of real equations. Overall, for a given pseudostate basis, the present approach requires more computational resources, but produces slightly more accurate results than the alternative approach studied in Ref. [23].

In the final analysis it is the nature of the two-particle approximation space s_α that is ultimately responsible for the success of the present approach as well as the successes of the alternative approaches studied Refs. [23,24]. In this respect it is critical that the primitive basis through which s_α is specified is chosen in the two-particle momentum space and has local compact support. Finite-element bases defined over an uneven momentum grid allow for efficient representation of breakup configurations. The p grids used in the present calculations are denser in the interval $0 < p < \sqrt{E/(2\mu)}$ than the rest. This feature makes it possible to obtain excellent results with 40–50 finite elements. Note that the transformation from primitive basis to pseudostate basis is performed solely for the purpose of isolating the open-channel singularities of the effective propagator in the corresponding diagonal elements.

Although the results obtained in this study were obtained by solving Eqs. (40) and (41) via quadrature discretization of the spectator momentum q, there are a large number of other possibilities. For example, the Bateman method could be considered in place of the Nyström method in order to reduce the computational burden somewhat. Of course, an L^2-basis discretization of the q variable is also a possibility. For instance, a Schwinger-type variational method could be used with a local basis in the q variable. In fact, one could invoke any one of a plethora of methods that exist for multichannel matrix LS equations in the literature [26,29,39]. A collection of projection/variational methods in the spirit of L^2 discretization with local momentum bases have been studied and tested in Refs. [26,29]. Especially some of the resolvent expansions studied in Ref. [29] may be relevant in the present context. If the propagator of the effective two-body equations is approximated by its projection in an L^2 subspace for the spectator, then the resulting computational scheme would amount to a complete L^2 discretization of the AGS equations, very similar to the approach taken in Refs. [27,28].

[1] L. D. Faddeev, Zh. Eksp. Teor. Fiz. **39**, 1459 (1960) [Sov. Phys. JETP **12**, 1014 (1961)].
[2] C. Lovelace, Phys. Rev. **135**, B1225 (1964).
[3] E. O. Alt, P. Grassberger, and W. Sandhas, Nucl. Phys. B **2**, 167 (1967).
[4] E. W. Schmid and H. Ziegelmann, *The Quantum Mechanical Three-Body Problem* (Pergamon, Oxford, 1974).
[5] W. Glockle, *The Quantum Mechanical Few Body Problem* (Springer, Berlin, 1983).
[6] A. N. Mitra, Nucl. Phys. **32**, 529 (1962).
[7] R. D. Amado, Phys. Rev. **132**, 485 (1963).
[8] A. N. Mitra and V. S. Bhasin, Phys. Rev. **132**, 986 (1963).
[9] E. Harms, Phys. Rev. C **1**, 1667 (1970).
[10] D. J. Ernst, C. M. Shakin, and R. M. Thaler, Phys. Rev. C **8**, 46 (1973).
[11] S. K. Adhikari, Phys. Rev. C **10**, 1623 (1974).
[12] S. K. Adhikari and I. H. Sloan, Phys. Rev. C **11**, 1133 (1975).
[13] Z. C. Kuruoglu and D. A. Micha, J. Phys. Chem. **72**, 3327 (1980).
[14] J. Haidenbauer and Y. Koike, Phys. Rev. C **34**, 1187 (1986).
[15] W. M. Kloet and J. A. Tjon, Ann. Phys. (NY) **79**, 407 (1973).
[16] N. M. Larson and J. H. Hetherington, Phys. Rev. C **9**, 699 (1974).
[17] V. M. Suslov and B. Vlahovic, Phys. Rev. C **69**, 044003 (2004).
[18] P. A. Belov and S. L. Yakovlev, Phys. At. Nucl. **76**, 126 (2013).
[19] J. L. Friar, B. F. Gibson, G. Berthold, W. Glöckle, Th. Cornelius, H. Witala, J. Haidenbauer, Y. Koike, G. L. Payne, J. A. Tjon *et al.*, Phys. Rev. C **42**, 1838 (1990).
[20] H. Witala, W. Glöckle, and T. Cornelius, Few-Body Syst. **3**, 123 (1988).
[21] E. Garrido, A. Kievsky, and M. Viviani, Phys. Rev. C **90**, 014607 (2014).
[22] Z. C. Kuruolu, Phys. Rev. C **44**, 1354 (1991).
[23] Z. C. Kuruoglu and F. S. Levin, Ann. Phys. (NY) **163**, 120 (1985).
[24] Z. C. Kuruoğlu, Few-Body Syst. **65**, 15 (2024).
[25] I. H. Sloan and J. T. Brady, Phys. Rev. C **6**, 701 (1972).
[26] Z. C. Kuruoğlu, Few-Body Syst. **55**, 1167 (2014).
[27] O. A. Rubtsova, V. N. Pomerantsev, V. I. Kukulin, and A. Faessler, Phys. Rev. C **86**, 034004 (2012).
[28] O. A. Rubtsova, V. I. Kukulin, and V. N. Pomerantsev, Ann. Phys. (NY) **360**, 613 (2015).
[29] Z. C. Kuruoğlu, Few-Body Syst. **55**, 69 (2014).
[30] P. M. Prenter, *Splines and Variational Methods* (Wiley, New York, 1975).
[31] Z. C. Kuruoğlu and F. S. Levin, Phys. Rev. A **46**, 2304 (1992).
[32] Z. C. Kuruoglu and F. S. Levin, Phys. Rev. Lett. **64**, 1701 (1990).
[33] Z. C. Kuruoğlu, Phys. Rev. C **101**, 024002 (2020).
[34] P. O. Löwdin, *Linear Algebra for Quantum Theory* (Wiley, New York, 1998).
[35] F. S. Levin, Phys. Rev. C **21**, 2199 (1980).
[36] Z. C. Kuruoglu and D. A. Micha, J. Chem. Phys. **80**, 4262 (1984).
[37] K. E. Atkinson, *A Survey of Numerical Methods for the Solution of Fredholm Integral Equations of the Second Kind* (SIAM, Philadelphia, 1976).
[38] J. L. Friar, G. L. Payne, W. Glockle, D. Huber, and H. Witala, Phys. Rev. C **51**, 2356 (1995).
[39] S. K. Adhikari, *Variational Principles and the Numerical Solution of Scattering Problems* (Wiley, New York, 1998).